

Article

Influence of Sequential Harvest on Chemical Composition of Merlot Wines

Anastazija Jež Kребelj ^{1,*}, Katja Šuklje ¹, Andreja Škvarč ², Mateja Potisek ¹  and Franc Čuš ¹ 

¹ Department of Fruit Growing, Viticulture and Oenology, Agricultural Institute of Slovenia, Hacquetova ulica 17, 1000 Ljubljana, Slovenia; katja.sukljeantalick@kis.si (K.Š.); mateja.potisek@kis.si (M.P.); franc.cus@kis.si (F.Č.)

² Slovene Chamber of Agriculture and Forestry, Institute of Agriculture and Forestry Nova Gorica, Vrhpolje 38/a, 5271 Vipava, Slovenia; andreja.skvarc@go.kgzs.si

* Correspondence: anastazija.jezkrebelj@kis.si

Abstract

The influence of grape maturity over three consecutive years (2020–2022) on Merlot (*Vitis vinifera* L.) juice and wine chemical composition was investigated. Grapes were harvested at three time points (H1, H2, and H3) in weekly intervals. Despite the fact that vintage (environmental conditions) had a predominant effect on juice and wine chemical composition, clear separation of samples according to the harvest date was observed in all three vintages. Compounds with the highest contribution towards harvest date separation were common maturity-related juice and wine variables (titratable acidity, pH) as well as some volatiles, whereas differences in total soluble solids between dates were minor and often insignificant. In particular, concentrations of 3-isobutyl-2-methoxypyrazine (IBMP), (Z)-3-hexenol, and 1-hexenol in wines decreased with delayed harvest. All the more, concentrations of 3-mercaptohexanol (3MH) were the lowest in wines from H3 in all three years, whereas concentrations of 3-mercaptohexyl acetate (3MHA) and 4-mercapto-4-methylpentan-2-ol (4MMP) were not influenced by harvest date. Other compounds, such as esters and higher alcohols, with the exception of 1-propanol, did not exhibit a common trend related to the harvest date across three vintages. These results indicate that, during late ripening, harvest-related shifts in juice and wine composition occur even when differences in berry sugar concentration (TSS) at harvest are minor.

Keywords: thiols; methoxypyrazines; grape maturity; chemical composition; vintage; harvest date; viticulture



Academic Editors: Alejandro Martinez Moreno, Diego Paladines-Quezada, Mario Cunha, Adamo Domenico Rombolà, Rajko Vidrih and Youssef Roupheal

Received: 17 November 2025

Revised: 16 January 2026

Accepted: 16 February 2026

Published: 20 February 2026

Copyright: © 2026 by the authors. Licensee MDPI, Basel, Switzerland. This article is an open access article distributed under the terms and conditions of the [Creative Commons Attribution \(CC BY\) license](https://creativecommons.org/licenses/by/4.0/).

1. Introduction

Grape aromatic potential is a result of complex interactions between grapevine genotype [1], environmental factors (such as climate and soil), agronomic practices [2,3], and grape maturity [4–10]. Decision on harvest dates is multifaceted [11] and typically relies on sugar concentration (TSS), titratable acidity (TA), pH, phenolic maturity, berry tasting, or berry sugar accumulation [11] in relation to potential wine style.

Sequential harvests represent an effective approach to modulate the development of aromas and flavors in young red wines [12–15]. The evolution of many compounds, such as terpenes [16,17], anthocyanins [18,19], and thiol precursors [20], has been shown to be closely related to grape ripening. However, recent studies suggest that similarities in accumulation patterns exist only until the slowdown of active sugar accumulation in the berries, which generally occurs between 18 and 20° Brix [21,22]. The later evolution of

the red wine aromatic profile is independent of further sugar accumulation in the grape berry [12]. The proposed aromatic evolution sequence, observed in Cabernet Sauvignon and Shiraz wines, develops from red-fruit aromas characteristic of early harvest dates to dark fruit and jammy aromas, common for wines from later harvest dates [11,12]. This progression reflects metabolic shifts occurring during late ripening that are no longer related to sugar accumulation [12,21]. Despite varietal differences, the potential evolution of red wine aromas during late ripening follows a similar aromatic pattern [22].

Interestingly, previous studies have demonstrated that, despite clear sensorial aromatic evolution and chemical separation of samples based on harvest date [12,17,23], only a limited number of reliable markers exist when comparing late and early harvest dates, which are all the more variety dependent [12,13]. This highlights complex interactions between several compounds in wine perception, with some present also in concentrations below the sensorial detection threshold. Beyond volatile aroma compounds, phenolic maturity and extractability also contribute to wine sensory properties during grape ripening in Merlot [24,25].

In this context, esters, which are primarily formed during fermentation, have been shown to be influenced by harvest date. In particular, higher alcohol acetates (HAAs) tend to increase with later harvest dates [12,13,23,26]. Since ester formation is closely linked to grape-derived substrates such as amino acids and fatty acids [27–29], harvest-related changes in grape composition may indirectly modulate fermentative aroma expression.

Similarly, grape-derived green-aroma compounds, including C6 alcohols and methoxypyrazines, exhibit pronounced ripening-dependent dynamics, providing additional markers of harvest timing effects on wine aroma [12,13,30]. A recent study conducted on single berries has demonstrated the evolution of C6 compounds in relation to TSS accumulation [31]. After an initial increase in monitored C6 compounds with TSS concentration, a decrease in late ripening per berry was observed [31], which is consistent with an increase in lipoxygenase-derived C6 compounds during early ripening, as observed in Riesling [32]. Although C6 aldehydes are the most abundant class of volatiles in grape berries, they are reduced to less abundant alcohols during fermentation [33]. In wines produced from sequentially harvested grapes, a decrease in (*Z*)-3-hexenol was observed in Shiraz [12] and Cabernet Sauvignon wines [13] with later harvest dates. A decreasing tendency with grape ripening was also observed for 3-isobutyl-2-methoxypyrazine (IBMP), a compound that typically contributes to green aromas, such as green pepper and tomato leaves, in several Bordeaux varieties [13,30,34].

Varietal thiols, 3-mercaptohexyl acetate (3MHA), 4-mercapto-4-methylpentan-2-ol (4MMP), and 3-mercaptohexanol (3MH), are considered as marker compounds of Sauvignon Blanc wines [35], even though they are often present in wines from various grape varieties above their sensorial detection threshold, which is 4 ng/L for 3MHA, 0.4 ng/L for 4MMP, and 60 ng/L for 3MH [36–38]. In red wines, the reported concentration ranges were lower for 3MHA and 4MMP [39] than those observed in Sauvignon Blanc wines, with concentration depending significantly on the grape origin and variety [40,41].

In the sub-Mediterranean climate, Merlot berries undergo rapid changes in sugars, acids, and phenolic compounds during ripening, making harvest timing a critical agronomic decision [4]. This study aimed to improve understanding of the dynamics of aroma evolution in Merlot wines associated with delayed harvest across climatically distinct vintages (e.g., warm dry versus mild wet) to contribute to the development of multi-parameter harvest criteria that extend beyond sugar accumulation alone [11,21,22]. Sequential harvesting enables a systematic assessment of how progressive grape maturity affects berry and wine metabolic composition [12]. Variations in metabolite profiles during ripening, together with known differences among cultivars grown under similar sub-Mediterranean

conditions, highlight the importance of the environment and cultivar interaction and the combined influence of genotype, vineyard site, and regional climate on wine style [14]. Integrating metabolomics with multi-set data analysis, including variance partitioning (VPA), principal component analysis, and random forest modelling, offers a robust framework for elucidating these abiotic drivers and enhancing our understanding of site expression in Merlot wine. Furthermore, understanding how sequential harvesting shapes the aromatic profile of wines [10,13] is essential for winemakers aiming to anticipate and strategically guide wine style outcomes [12,15]. To date, research on sequential harvest has mainly been restricted to Cabernet Sauvignon and Shiraz [12–15,18–21], often limited to a single vintage and without a comprehensive evaluation of varietal thiols [40,41]. Consequently, the relative influence of vintage and harvest timing on Merlot aroma compounds in sub-Mediterranean vineyards is still insufficiently understood. In this context, we selected three sequential harvest dates, with the first harvest date (H1) corresponding to the onset of technological maturity, followed weekly by H2 and H3, to test the hypothesis that delayed harvest modulates juice and wine chemical composition in a vintage-dependent manner. This study therefore presents an integrated multi-vintage assessment of Merlot juice, and wine composition across three harvest dates and three vintages under sub-Mediterranean climatic conditions.

2. Materials and Methods

2.1. Vineyard Site and Grape Sampling

Merlot (clone candidate 'G1-3') (*Vitis vinifera* L.) grapes were harvested in three consecutive vintages, i.e., 2020, 2021, and 2022, from an experimental vineyard located in Vipava Valley, Primorska, Slovenia (45°50'03.4'' N, 13°56'18.8'' E). Vines were grafted on Kober 5BB rootstock and planted in 2014 with row orientation west-east and spacing of 2.5 m between rows and 1.0 m between vines; ~4000 vines per hectare. The vineyard was moderately sloped with an average inclination of 8%. Vines were trellised to a single Guyot (on average 12 buds per vine retained after winter pruning) and not irrigated.

The inter-row surface was maintained with permanent grass cover and mulched during the season, whereas under the row was mechanically cultivated to control grass, with no use of herbicides. An experimental plot of 25 vines per replicate was established across three rows in the middle of the experimental vineyard. Each replicate consisted of 25 adjacent vines. Basic agronomical traits (number of shoots per vine, number of fertile shoots per vine, yield/vine, number of bunches/vine, bunch weight, and Ravaz index) were assessed on 10 vines per replicate, seasonally. Phenological development was monitored using the BBCH scale [42]. Phenological stages that were monitored on 30 vines included budburst (sprouting) (BBCH 07–09), recorded when 50% of the buds reached the green shoot tip stage; leaf development/ Inflorescence emergence (BBCH 13–15/53–58); flowering (BBCH 60–68), assessed when a defined percentage of flowers were open; development of fruits (BBCH 77); and the onset of ripening (BBCH 85), observed when berries began to soften. Each stage was recorded when approximately 50% of the plants had reached the corresponding developmental phase.

Grape maturity was assessed weekly from BBCH 88 onwards on representative vines by measuring TSS, TA, pH, and berry fresh mass. For each assessment, 100 berries were collected from different positions within the canopy to obtain a representative sample. The first harvest date (H1) coincided with technological maturity determined based on berry mass, TSS, TA concentration, and pH value. Subsequent harvests (H2 and H3) were scheduled at 7-day intervals after H1 to capture compositional changes associated with delayed harvest. In 2020, H1, H2, and H3 were carried out on the 16th, 22nd, and 29th of September, corresponding to 110, 116, and 123 days after anthesis (DAA), respectively.

In 2021, harvests were performed on 15th, 22nd, and 28th September (99, 106, and 112 DAA, respectively), and in 2022 on 1st, 7th, and 14th September, corresponding to 96, 102, and 109 DAA, respectively (Table 1). For each harvest date, approximately 30 kg of grapes per replicate were harvested from 10 randomly selected vines, with the exception of 2022, where yield was reduced up to 50% due to drought as compared to the previous two years. Harvested grapes were immediately transported into the experimental wine cellar, where they were stored at +4 °C, overnight until processed the following day.

Table 1. Harvest dates, days after anthesis (DAA), and growing degree days (GDD₁₀) for each harvest point in the years 2020, 2021, and 2022.

Year	Harvest Point	Harvest Date	DAA	GDD ₁₀
2020	H1	16.09.2020	110	1841
	H2	22.09.2020	116	1904
	H3	29.09.2020	123	1946
2021	H1	15.09.2021	99	1751
	H2	22.09.2021	106	1811
	H3	28.09.2021	112	1862
2022	H1	1.09.2022	96	1930
	H2	7.09.2022	102	2001
	H3	14.09.2022	109	2073

2.2. Weather Conditions

Meteorological data were collected from the Agrometeorological Portal of Slovenia UVHVVR (available online: <http://agromet.mkgp.gov.si/APP2/Detail?id=255&archive=> (accessed on 13 April 2023)) from the Slap weather station (49193), located 60 m from the experimental vineyard (45°50′01.7″ N 13°56′21.9″ E)). Average temperatures and precipitation for the period from 1 April to 30 September for the 2020, 2021, and 2022 vintages were calculated (Figure 1). The growing degree days (GDD₁₀) were calculated using 10 °C as the baseline temperature for the grapevine, which was subtracted from the daily average temperatures recorded from April 1 to each harvest date [43]. The Huglin index was calculated from 1 April to 30 September as described [44]. All temperature data are expressed in °C.

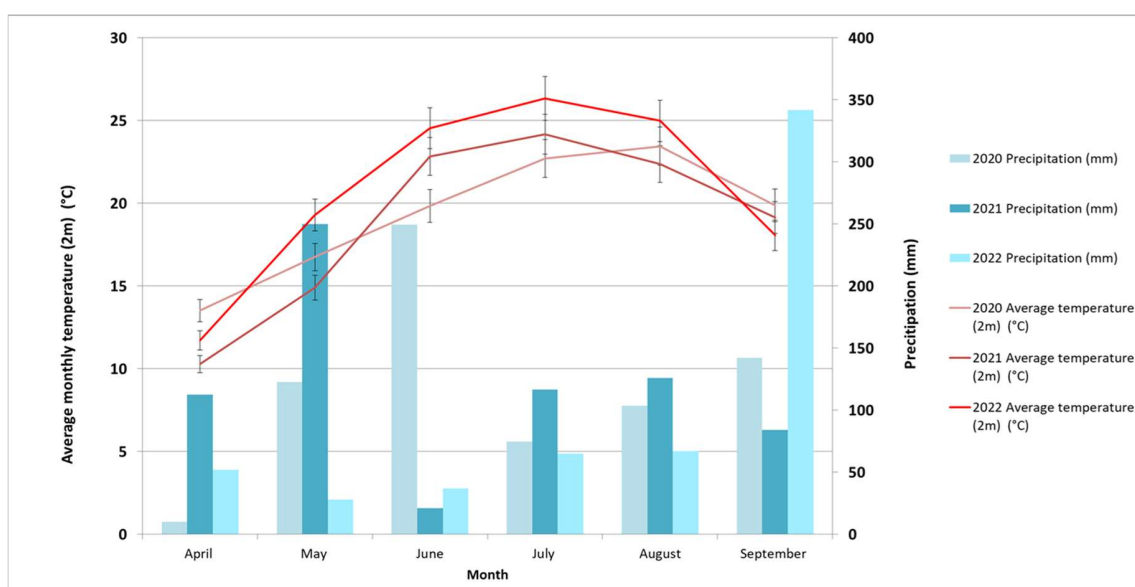


Figure 1. Average monthly temperatures (°C)—lines and precipitation (mm)—histograms from April to September in 2020, 2021, and 2022 (Slap, Slovenia).

2.3. Small-Scale Vinifications

The day after harvest, grapes were destemmed using an Inox destemmer (Enoop, Vipava, Slovenia). The grape mash was placed into a 15 L glass vessel, and the weight of the fermenter was adjusted to approximately 10 kg. Additionally, 0.2 mL/L SO₂ (as a 5–6% aqueous solution of sulphurous anhydride, Agrolit, Slovenia) was added to each fermenter to prevent oxidation and stirred. Fifty milliliters of juice were taken for analysis of TSS, TA, and pH. Commercial yeast *Saccharomyces cerevisiae* RX60 (Lallemand, Montreal, QC, Canada) was added to the grape mash at a rate of 0.3 g/L without prior rehydration after the grape mash had reached 18 °C. Fermentations were carried out in a temperature-controlled room at 22 °C (±2 °C). Punching down was performed twice daily. At about one-third of fermentation, as determined by refractometric TSS measurements, yeast nutrient Nutristart Org (Laffort, France) at a dose of 0.3 g/L, corresponding to an addition of 30 mg of yeast assimilable nitrogen (YAN) (mg N/L), was added. The progress of fermentation was monitored daily by refractometric measurements. All treatments fermented to a residual sugar content of 1.1–1.5 g/L, measured with an enzymatic robot (Mindray BS-200; Shenzhen Mindray Bio-Medical Electronics Co., Ltd., Shenzhen, China). Grape mash was pressed with a small manual press after 10 days of maceration. Pressed wines were kept at 22 °C to complete alcoholic and malolactic fermentation (MLF). At the end of MLF, measured with an enzymatic robot, 1.0 mL/L of a 5–6% aqueous solution of sulphurous anhydride (Agrolit, Slovenia) was added, and the wines were racked. The wines were bottled 8 to 10 weeks after the first racking into 0.75 L screw-cap bottles and stored at 12 °C until analysis.

2.4. Basic Analysis of Juice and Wine

The TSS in the juice was determined using a digital refractometer WM-7 (Atago, Saitama, Japan). The pH values of juice and wine were measured using a MeterLab PHM 210 (Radiometer Analytical, Lyon, France). Juice TA was determined by sodium hydroxide titration with bromothymol as the indicator for the colorimetric modification and expressed as g/L tartaric acid. Reducing sugars in wine was quantified using an enzymatic robot (BS-200, Mindray, Nanshan, Shenzhen, China), and total dry matter was determined using the method OIV-MA-AS2-03B. Alcohol content in wine was measured using an AlcoLyzer Wine M alcohol meter (Anton Paar, Graz, Austria).

2.5. Analysis of Anthocyanins and Polyphenols

Total anthocyanins and polyphenols in wine samples were analyzed spectrophotometrically using an Agilent 8453 spectrophotometer (Agilent Technologies Inc., Palo Alto, CA, USA), as described previously [45,46]. Prior to analysis, polar compounds (sugars, free SO₂, amino acids, and organic acids) were removed from the wines using Sep-Pak C-18 columns (0.5 g, Waters Corporation Milford, Milford, MA, USA). Total anthocyanins were determined based on the maximum absorbance in the visible range between 536 and 542 nm. Total polyphenols, expressed as (+)-catechin in mg/L, were estimated by Folin–Ciocalteu reagent reduction to blue pigments due to the phenols in the alkaline solution.

2.6. Analyses of Varietal Thiols

Thiols in wines (4MMP, 3MH, and 3MHA) were extracted using Dowex ionic resin, according to the method described by [47], with slight modifications in sample preparation [48]. Briefly, 50 mL of wine sample was spiked with internal standards: 4-methoxy-2-methyl-2-mercaptobutane (Sigma Aldrich, Schnelldorf, Germany) for 4MMP quantification, and d5-3-mercaptohexan-1-ol (Eptes, Switzerland) for 3MH and 3MHA quantification. After adjusting the wine pH value to 7, samples were passed through a Dowex resin and then eluted with cysteine buffer as described in [47,48]. Thiols were

extracted from the cysteine buffer using liquid-liquid extraction with ethyl acetate and dichloromethane. The organic phase was collected, dried over anhydrous sodium sulfate, and concentrated to a final volume of 50 μ L. Samples were analyzed as described [48], using a gas chromatograph (GC) (Agilent Technologies 7890A, Palo Alto, CA, USA) coupled to a mass spectrometer (Agilent Technologies 5975C, Palo Alto, CA, USA). The chromatograph was equipped with a capillary column (Agilent J&W GC column: HP-INNOWAX, 60 m \times 0.25 mm; film thickness 0.25 μ m). Helium was used as a carrier gas at a constant flow rate of 0.6 mL/min. The injector temperature was set to 240 $^{\circ}$ C with an oven temperature gradient of 50 $^{\circ}$ C for 5 min, then from 50 $^{\circ}$ C to 115 $^{\circ}$ C at 3 $^{\circ}$ C/min, then from 115 $^{\circ}$ C to 150 $^{\circ}$ C at 40 $^{\circ}$ C/min, 3 min at 150 $^{\circ}$ C, then from 150 $^{\circ}$ C to 205 $^{\circ}$ C at 3 $^{\circ}$ C/min, from 205 $^{\circ}$ C to 250 $^{\circ}$ C at 10 $^{\circ}$ C/min, 19.625 min at 250 $^{\circ}$ C, then back from 250 $^{\circ}$ C to 50 $^{\circ}$ C at 40 $^{\circ}$ C/min, and 3 min at 50 $^{\circ}$ C. The ion source temperature was 230 $^{\circ}$ C, the auxiliary temperature was 250 $^{\circ}$ C, and the quadrupole temperature was 150 $^{\circ}$ C [48]. One-point calibration was performed using calibration standards in an alcoholic solution with a final concentration of 65 ng/L 4MMP, 650 ng/L 3MHA, and 1202 ng/L 3MH and injected after every ninth sample. The limit of quantification (LOQ) was 2, 4, and 60 ng/L for 4MMP, 3MHA, and 3MH, respectively [49,50].

2.7. Analyses of Methoxypyrazines

Methoxypyrazines, specifically IBMP and 3-isopropyl-2-methoxypyrazine (IPMP) in wines, were quantified by GC-MS (Agilent Technologies, Palo Alto, CA, USA) equipped with a Gerstel MPS2 multifunctional sampler (Gerstel, Muelheim an der Ruhr, Germany) as described [51]. Briefly, to a 20 mL headspace (HS) vial, 3 g of NaCl was added, followed by 1.6 mL of wine, 6.4 mL of MilliQ water, and 2 mL of 4M NaOH. An internal standard, d5-3-isobutyl-2-methoxypyrazine (C/D/N Isotopes, Quebec, Canada), was added to reach the final concentration of 25 ng/L. Analytes were extracted on grey fiber DVB/CAR/PDMS (Supelco, Bellefonte, PA, USA) for 40 min at 40 $^{\circ}$ C and separated on successively connected columns, an HP 1 MS (Agilent Technologies, 30 m, 0.32 mm i.d., 0.25 μ m film thickness) and an HP INNOWAX (Agilent Technologies, 30 m, 0.32 mm i.d., 0.25 μ m film thickness), with a constant flow of helium at 1.5 mL/min as described [51].

2.8. Analysis of Higher Alcohols, Ethyl Acetate, Acetaldehyde, and Diethylacetal

Higher alcohols, ethyl acetate, acetaldehyde, and diethylacetal were analyzed using GC coupled to a flame ionization detector (FID) (Hewlett Packard 6890, Hewlett-Packard GmbH, Waldbronn, Germany) without previous extraction using CP-Wax, 57CB, 50 m \times 0.25 mm, film thickness 0.20 μ m column (Agilent Technologies, Palo Alto, CA, USA) as described [52]. A 5 mL wine sample was spiked with the internal standard 4-methyl-2-pentanol (Sigma Aldrich), vortexed, and 1 μ L was directly injected into the GC-FID. Validation of the method was carried out as described [53], and quantification was performed as previously reported [52,53].

2.9. Analysis of Esters, 1-Hexenol, (Z)-3-Hexenol, γ -Butyrolactone, and Benzyl Alcohol

Esters, C6 alcohols, and other compounds were analyzed as previously described [53] following liquid-liquid extraction with dichloromethane and organic phase concentration to 1 mL, as described in [53]. Samples were analyzed using GC (Hewlett Packard 6890, Waldbronn, Germany), coupled to an MS (Hewlett Packard 5973, Palo Alto, CA, USA), using a CP-Wax 57CB 50 m \times 0.25 mm, film thickness 0.20 μ m Varian (Lake Forest, CA, USA) column, coupled to a fused silica deactivated 2 m \times 0.25 mm guard column (Agilent Technologies, Palo Alto, CA, USA). Compound identification and quantification were performed as described in [52,53].

2.10. Statistical Analysis

Statistical analyses were performed using Statistica, version 12 (StatSoft, Tulsa, OK, USA). The Shapiro–Wilk normality test was used to assess the normality of the data, while the homogeneity of variances was tested using the Levene test. For variables with a normal distribution, one-way ANOVA was applied to test the influence of harvest date on the variables studied in juice and wine, followed by Tukey’s test for means separation. For variables with non-homogeneous variances and non-normal distribution, the non-parametric Kruskal–Wallis test was used, and means were separated using the Dunn’s test. Two-way ANOVA was applied to test the interaction between harvest date and vintage on the variables studied in juice and wine. Different letters indicate significant differences at $p \leq 0.05$. Asterisks indicate the significance level: * $p \leq 0.05$, ** $p \leq 0.01$, and *** $p \leq 0.001$. To quantify the contribution of vintage and harvest date to wine and grape variables, VPA was performed in RStudio v2023.09.1 (RStudio Team, 2012). Key metabolites influenced by harvest date were determined using random forest analyses in RStudio, and heatmaps were generated using the pheatmap package in RStudio v2023.09.1 (RStudioTeam, 2012). The factoextra and ggplots packages in RStudio v2023.09.1 (RStudioTeam, 2012) were used to perform principal component analysis (PCA) on log₂-transformed data that were Z-scaled for each vintage individually to minimize the effect of vintage [17].

3. Results

3.1. Seasonal Weather Conditions

The experiment was carried out in three climatically distinctly different vintages. The calculated Huglin index for the experimental site in 2021 was 2385 units, indicating that the vintage was classified as temperate-warm [44]. The vintages of 2020 and 2022, with calculated Huglin indexes of 2407 and 2680 units, respectively, were classified as warm [44]. Important differences between vintages were observed in average monthly temperatures (Figure 1). The largest difference, 4.7 °C, was recorded in June 2022 compared to 2020, with 2022 being the warmer of the two years (Figure 1).

Vintages 2020 and 2021 were characterized by higher precipitation. During the 2020 and 2021 growing seasons (April–September), a total of 703 and 710 mm of rainfall was recorded, with precipitation peaks occurring in June 2020 (249.4 mm) and May 2021 (249.8 mm), respectively. In 2022, a total of 590.6 mm of precipitation was recorded for the April–September period, of which 294.8 mm fell in September, after the last harvest date. The 2022 vintage was characterized by low precipitation and high temperatures; maximum daily temperatures between 27 June and 6 August exceeded 35 °C on 15 days in total during that period. This led to accelerated grape ripening and an earlier harvest by 14 days compared to 2020 and 2021. Also, accumulated GDD₁₀ were significantly higher at all three harvest dates in 2022 compared to previous vintages (Table 1).

3.2. Influence of Harvest Date on Grape and Wine Composition

To assess the overall influence of vintage and harvest date on the chemical composition of Merlot grape juice and wine, VPA analyses were performed on all measured juice variables and wine metabolites. The results showed that 60% of the variation in juice and wine composition could be explained by the combined effect of vintage and harvest date (Figure 2). Vintage accounted for 49% of the variation, while 11% of the variation was explained by harvest date (Figure 2).

For the PCA (Figure 3A,B), variables were z-scaled within each vintage; therefore, harvest-related differences are emphasized rather than between-vintage absolute shifts (Figure 2). The PCA revealed distinct clustering patterns associated with the three harvest dates (Figure 3A). Samples from each harvest, irrespective of vintage, formed well-defined

groups, demonstrating that the chemical composition of both juice and the resulting wines differed systematically with harvest time.

The PCA loading plot (Figure 3B) shows that later harvest dates aligned positively with the first principal component (PC1) together with pH_{juice} and TSS, while being negatively correlated with several higher alcohols and IBMP (Figure 3B). Some fermentation-derived volatiles (e.g., ethyl acetate and 2-phenethyl acetate) also loaded positively on PC1, although ester responses were vintage dependent and not consistently monotonic across harvest dates.

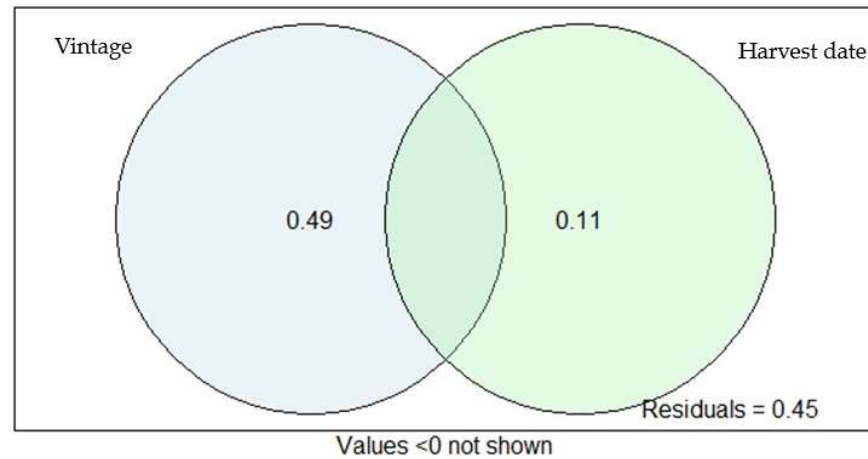


Figure 2. Variance partitioning analyses (VPA) show the contribution of vintage and harvest date and their interaction to the variability of Merlot grape juice and wine composition.

Random forest analysis was used to rank compounds according to their discriminatory power between harvest dates (Figure 4A,B). Titratable acidity in grape juice (juice TA) was identified as the parameter that differed the most between three harvest dates, displaying the highest mean decrease in Gini (Figure 4A). The next most significant variables were 1-hexanol and wine pH. The remaining variables, γ -butyrolactone, (Z)-3-hexen-1-ol, ethanol, 1-propanol, diethyl succinate, IBMP, and 3MH, had broadly similar importance values, implying that they contribute comparably but to a lesser extent than TA_{juice} (Figure 4A).

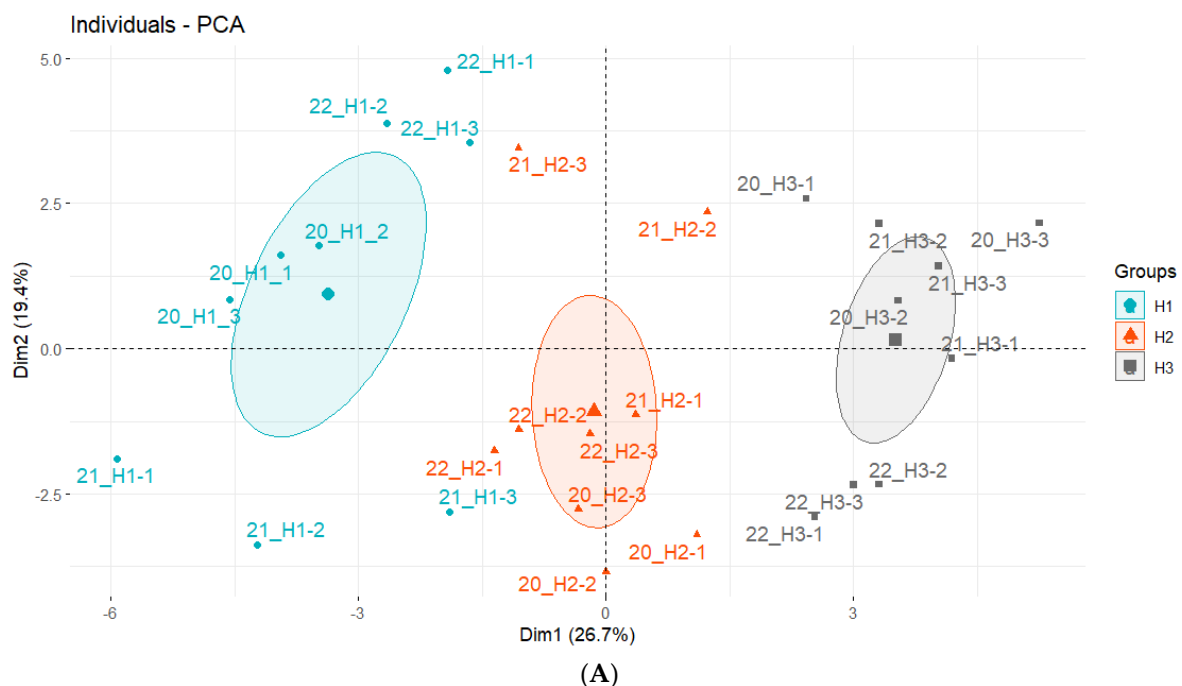


Figure 3. Cont.

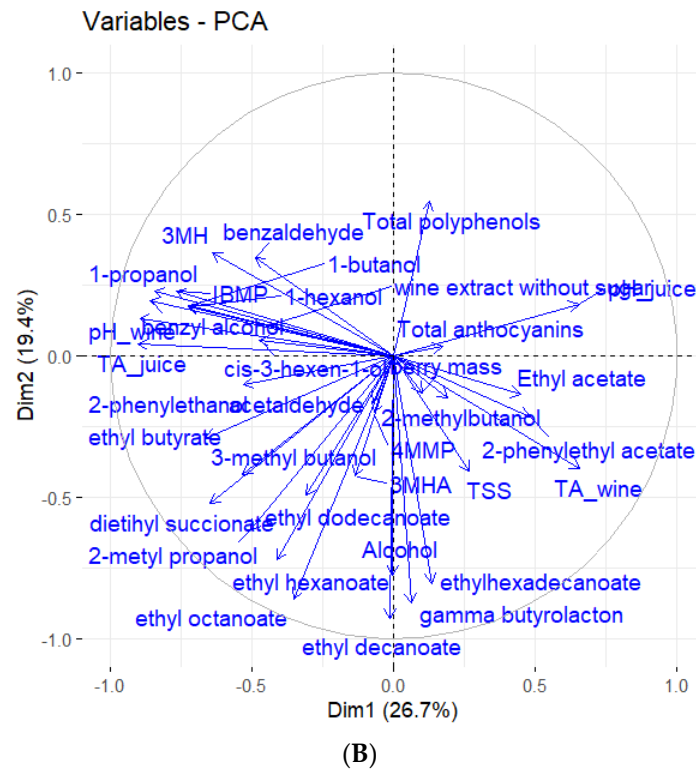


Figure 3. (A) Principal component analysis of Merlot juice and wine variables listed in Table 3 according to harvest time (H1–H3). Scores of principal component analyses (PCA) for the first two dimensions conducted on log2 transformed and z-normalized data. Abbreviations of the groups H1 (blue), H2 (red), and H3 (grey) refer to the first, second, and third harvest dates, respectively, for the 2020, 2021, and 2022 vintages. Ellipses represent the 95% confidence intervals for sample groups. (B) PCA loading plot showing the contribution of grape juice, and wine variables to the first two principal components. Longer arrows represent variables with a higher contribution to the total variance.

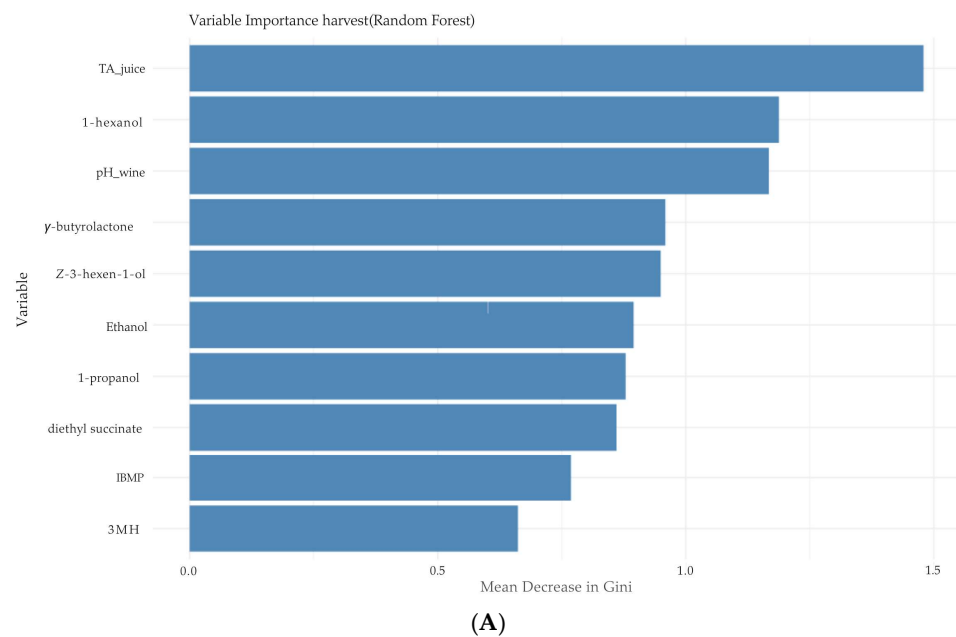
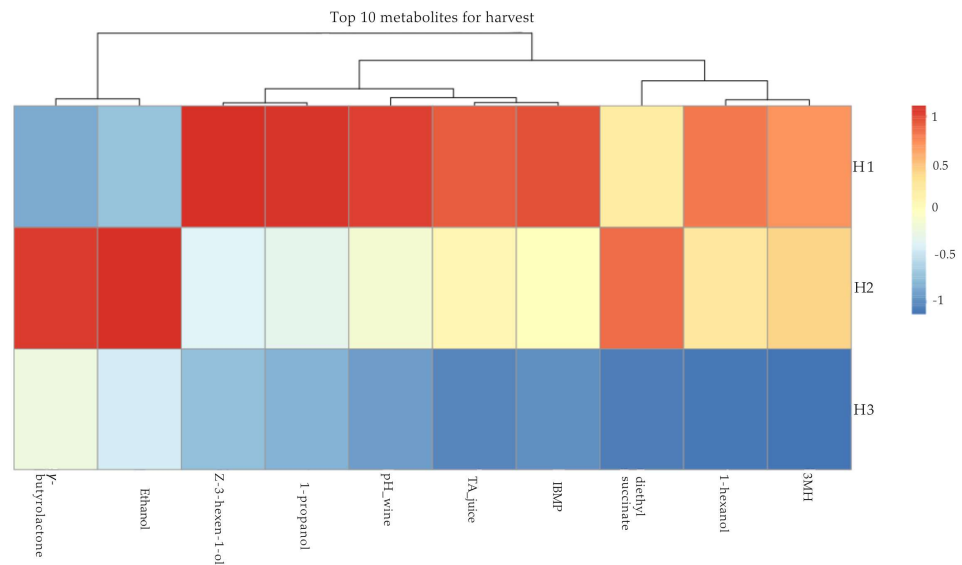


Figure 4. Cont.



(B)

Figure 4. (A) Random forest analyses for the grape juice and wine variables across vintages for harvest dates. The ten most important variables are ranked according to their importance, expressed as the mean decrease in the Gini index. (B) Heatmap of ten most important variables in Merlot grape juice and wine as identified by random forest analyses illustrating differences among harvest dates (H1–H3).

The heatmap of the top ten variables identified by random forest analyses (Figure 4B) shows clear differences in chemical profiles among the three harvest dates (H1–H3). Harvest date H1 was associated with 3MH, 1-hexanol, TA_juice, pH_wine, and IBMP, whereas H2 was associated with diethyl succinate, ethanol, and γ -butyrolactone. Absolute concentrations of variables shown in the heatmap across harvest dates and vintages are presented in Tables 2 and 3.

Table 2. Juice composition and yield parameters for three harvest dates in the 2020, 2021, and 2022 vintages. Data are presented as mean \pm SD (n = 3). Letters in the same column indicate statistically significant differences, determined by one-way ANOVA followed by Tukey’s and Dunn’s (marked as †) post-hoc test. Two-way ANOVA was applied to test the interaction between harvest date and vintage. Asterisks indicate the significance level: ** $p \leq 0.01$, and *** $p \leq 0.001$ for harvest date (H), vintage (V), and interaction between harvest date and vintage (H \times V).

Variable	Harvest Date	Vintage			p-Values		
		2020	2021	2022	H	V	H \times V
Juice TSS ($^{\circ}$ Brix)	H1	22.6 \pm 0.1 ^b	22.5 \pm 0.2	23.2 \pm 0.0 ^b	**	***	ns
	H2	22.9 \pm 0.1 ^a	23.0 \pm 0.7	24.0 \pm 0.2 ^a			
	H3	22.8 \pm 0.1 ^a	22.3 \pm 0.4	23.5 \pm 0.3 ^b			
Juice pH	H1	3.57 \pm 0.01 ^b	3.47 \pm 0.03 ^c	3.69 \pm 0.02	***	***	***
	H2	3.47 \pm 0.04 ^c	3.56 \pm 0.01 ^b	3.77 \pm 0.03			
	H3	3.74 \pm 0.02 ^a	3.62 \pm 0.02 ^a	3.75 \pm 0.05			
Juice TA (g/L)	H1	5.8 \pm 0.4 ^{a,†}	5.2 \pm 0.1 ^a	3.8 \pm 0.1 ^b	***	***	***
	H2	4.3 \pm 0.1 ^b	4.4 \pm 0.3 ^b	4.3 \pm 0.8 ^a			
	H3	4.1 \pm 0.1 ^b	3.6 \pm 0.0 ^c	2.8 \pm 0.1 ^c			
Berry mass (g)	H1	1.55 \pm 0.06	1.64 \pm 0.11	1.13 \pm 0.3 ^b	ns	***	**
	H2	1.45 \pm 0.07	1.68 \pm 0.06	1.10 \pm 0.07 ^b			
	H3	1.37 \pm 0.08	1.67 \pm 0.02	1.26 \pm 0.05 ^a			
Yield/vine (kg)	H1	4.01 \pm 0.55	3.43 \pm 1.00	2.01 \pm 0.52	ns	***	ns
	H2	3.97 \pm 1.09	3.57 \pm 1.07	1.62 \pm 0.56			
	H3	3.59 \pm 1.05	3.31 \pm 1.19	2.06 \pm 0.42			

Table 3. Wine chemical composition for three harvest dates (H1, H2, and H3) in the 2020, 2021, and 2022 vintages. Data are presented as mean ± standard deviation (n = 3), letters in the same row indicate statistically significant differences, Tukey's and Dunn's (marked as †) post-hoc test. Asterisks indicate the significance level: * p ≤ 0.05, ** p ≤ 0.01, and *** p ≤ 0.001 for between harvest date (H), vintage (V), and interaction between harvest date and vintage (H × V).

Year	2020			2021			2022			p-Values		
Harvest Date	H1	H2	H3	H1	H2	H3	H1	H2	H3	H	V	H × V
Basic wine variables												
Ethanol (% vol)	13.4 ± 0.0 ^b	14.0 ± 0.1 ^a	13.3 ± 0.2 ^b	13.7 ± 0.2	13.7 ± 0.5	13.5 ± 0.1	13.4 ± 0.0 ^b	14.2 ± 0.1 ^a	14.0 ± 0.1 ^a	**	ns	*
pH	3.98 ± 0.01 ^a	3.91 ± 0.04 ^b	3.81 ± 0.03 ^c	3.97 ± 0.04 ^a	3.89 ± 0.04 ^b	3.85 ± 0.01 ^b	3.87 ± 0.01 ^{a,†}	3.77 ± 0.01 ^{b,†}	3.76 ± 0.02 ^{b,†}	***	***	ns
TA (g/L)	3.8 ± 0.3 ^b	4.5 ± 0.2 ^a	4.8 ± 0.2 ^a	4.7 ± 0.3	4.7 ± 0.2	4.8 ± 0.1	4.3 ± 0.1	4.5 ± 0.1	4.5 ± 0.1	***	**	**
Total dry matter (g/L)	27.2 ± 0.9	27.0 ± 0.3	27.5 ± 0.3	27.1 ± 0.2	26.9 ± 0.6	26.2 ± 0.3	31.2 ± 1.0 ^a	31.3 ± 1.3 ^a	29.3 ± 0.1 ^b	*	***	*
Total polyphenols and anthocyanins												
Total polyphenols ((+)-Catechin) (mg/L)	1125.0 ± 47.2 ^b	1055.2 ± 83.5 ^b	1335.3 ± 36.2 ^a	1062.3 ± 51.6 ^b	1315.5 ± 34.5 ^a	1127.7 ± 7 ^b	1386.5 ± 13.8	1385.5 ± 178.6	1236.4 ± 110.7	ns	**	***
Total anthocyanins (mg/L)	568.7 ± 3.5 ^b	633.8 ± 17.9 ^a	673.6 ± 45.6 ^a	659.0 ± 18.8	724.6 ± 68.6	680.0 ± 121.2	695.8 ± 14.9	739.8 ± 62.6	651.0 ± 7.4	ns	*	ns
Wine volatiles												
Varietal thiols (ng/L)												
4MMP	6.36 ± 0.72	9.9 ± 6.69	8.07 ± 2.18	4.37 ± 2.56	3 ± 0.75	2.67 ± 1.02	LD	LD	LD	ns	ns	ns
3MHA	17.59 ± 3.77	23.01 ± 2.88	19.58 ± 3.43	11.73 ± 2.68	7.1 ± 1.73	6.67 ± 2.01	23.09 ± 4.20	24.85 ± 20.47	29.59 ± 0.07	ns	**	ns
3MH	1230.52 ± 72.98 ^a	948.17 ± 62.72 ^b	811.12 ± 145.49 ^b	619.97 ± 36.18 ^b	865.03 ± 50.90 ^a	530.09 ± 78.15 ^b	733.85 ± 29.72 ^a	671.58 ± 41.97 ^b	609.11 ± 17.35 ^b	***	***	***
Methoxyppyrazine (ng/L)												
IBMP	6.57 ± 0.42 ^a	4.00 ± 0.80 ^b	4.93 ± 1.39 ^b	2.68 ± 0.16 ^a	2.22 ± 0.32 ^b	1.83 ± 0.13 ^b	4.80 ± 1.56 ^a	4.33 ± 2.61 ^a	0.23 ± 0.40 ^b	**	***	*
Alcohols (mg/L)												
1-Propanol (-)	24.68 ± 0.18	18.20 ± 0.71	18.81 ± 1.81	30.97 ± 4.24	23.02 ± 1.54	23.01 ± 0.89	43.88 ± 2.18 ^a	41.65 ± 3.39 ^a	35.03 ± 1.74 ^b	***	***	ns
2-Methyl-1-propanol	55.4 ± 0.2 ^a	52.12 ± 1.11 ^b	46.78 ± 0.92 ^c	49.11 ± 2.04 ^a	45.38 ± 0.89 ^b	43.8 ± 0.94 ^b	45.63 ± 0.59 ^b	50.50 ± 1.12 ^a	52.12 ± 0.60 ^a	**	***	***
1-Butanol	1.48 ± 0.12 ^a	1.15 ± 0.12 ^b	1.09 ± 0.11 ^b	1.70 ± 0.19	1.84 ± 0.09	1.54 ± 0.08	2.11 ± 0.13 ^a	2.32 ± 0.30 ^a	1.72 ± 0.04 ^b	***	***	**
2-Methyl-1-butanol	69.66 ± 0.18 ^a	61.97 ± 0.75 ^b	65.74 ± 2.55 ^a	67.10 ± 1.07	66.90 ± 1.51	68.40 ± 0.97	58.47 ± 4.19 ^b	66.9 ± 2.22 ^a	69.33 ± 1.35 ^a	*	ns	***
3-Methyl-1-butanol	247.08 ± 3.44 ^a	204.04 ± 6.55 ^b	201.45 ± 10.85 ^b	237.43 ± 2.64 ^a	220.77 ± 6.51 ^b	215.64 ± 6.02 ^b	226.68 ± 10.61	237.64 ± 3.2	237.86 ± 5.38	***	***	***
2-Phenylethanol	43.26 ± 1.27	37.83 ± 3.13	38.92 ± 2.49	51.61 ± 2.30 ^a	48.83 ± 0.61 ^{a,b}	47.15 ± 0.89 ^b	38.89 ± 3.35	41.92 ± 5.6	39.31 ± 4.15	*	***	ns
1-Hexanol	2.30 ± 0.17	2.27 ± 0.15	1.30 ± 0.10	1.55 ± 0.06 ^a	1.61 ± 0.03 ^a	1.41 ± 0.07 ^b	2.76 ± 0.11 ^a	2.11 ± 0.18 ^b	1.80 ± 0.17 ^c	***	***	***
(Z)-3-hexen-1-ol	0.01 ± 0.00	0.02 ± 0.00	0.01 ± 0.00	0.02 ± 0.00 ^a	0.01 ± 0.00 ^b	0.01 ± 0.00 ^b	0.03 ± 0.00 ^{a,†}	0.02 ± 0.00 ^{b,†}	0.02 ± 0.00 ^{b,†}	***	***	***
Benzyl alcohol	2.54 ± 0.21 ^a	1.93 ± 0.05 ^b	1.31 ± 0.24 ^c	0.88 ± 0.09 ^a	0.66 ± 0.12 ^b	0.61 ± 0.05 ^b	1.06 ± 0.02 ^a	0.83 ± 0.10 ^b	0.66 ± 0.01 ^c	***	***	***
SUM alcohols	446.41 ± 3.87	379.52 ± 9.56	375.42 ± 15.83	440.37 ± 8.54	409.01 ± 6.12	401.55 ± 8.25	419.52 ± 14.5	443.89 ± 5.76	437.85 ± 3.56			
Ethyl esters of strain chain fatty acids (EEFAs) (µg/L)												
Ethyl butyrate	169.33 ± 5.77	151.67 ± 2.31	131.00 ± 32.36	246.67 ± 10.26 ^a	174.67 ± 17.67 ^b	175.33 ± 5.03 ^b	140.77 ± 24.79	150.34 ± 23.87	129.03 ± 40.32	**	***	*
Ethyl hexanoate	320 ± 17.32 ^a	336.67 ± 15.28 ^a	263.33 ± 20.82 ^b	248.67 ± 27.39	202.00 ± 15.87	210.67 ± 12.50	279.93 ± 8.10	310.90 ± 10.02	310.59 ± 33.26	ns	***	***
Ethyl octanoate	356.67 ± 5.77 ^a	366.67 ± 5.77 ^a	316.67 ± 15.28 ^b	300 ± 22.87 ^a	223.33 ± 26.58 ^b	234.67 ± 29.48 ^b	282.68 ± 13.91 ^{b,†}	394.90 ± 1.11 ^{a,†}	383.31 ± 9.01 ^{a,†}	ns	***	***
Ethyl decanoate	81.00 ± 1.00 ^b	101.33 ± 2.08 ^a	81.67 ± 8.08 ^b	53.33 ± 6.51 ^a	39.00 ± 5.20 ^b	40.00 ± 6.24 ^b	54.89 ± 2.31 ^c	74.82 ± 2.65 ^b	92.99 ± 6.45 ^a	**	***	***
Ethyl dodecanoate	5.67 ± 3.06	8.67 ± 0.58	5.33 ± 1.53	8.67 ± 0.58	7.67 ± 1.53	6.33 ± 0.58	LD	LD	LD	/	/	/
Ethyl hexadecanoate	7.67 ± 0.58 ^b	20.00 ± 6.00 ^a	15.00 ± 5.29 ^a	50.00 ± 6.56	36.00 ± 20.81	29.00 ± 7.81	22.02 ± 4.17 ^b	38.93 ± 6.29 ^a	34.46 ± 2.16 ^a	ns	***	*
SUM EEFAs	940.33 ± 33.50	985 ± 32.02	813 ± 83.35	907.33 ± 74.17	682.67 ± 87.66	696 ± 61.65	780.29 ± 53.29	969.88 ± 43.94	950.38 ± 91.21			
Other compounds												
Benzaldehyde (µg/L)	26.20 ± 9.11	8.33 ± 0.58	12.40 ± 7.38	2.77 ± 0.60	2.03 ± 0.15	2.83 ± 0.49	2.04 ± 0.20	1.89 ± 0.17	1.65 ± 0.16	*	***	**
Diethyl succinate (mg/L)	5.80 ± 0.00 ^{b,†}	8.83 ± 0.31 ^{a,†}	0.70 ± 0.10 ^{c,†}	1.70 ± 0.17 ^a	1.02 ± 0.17 ^a	0.71 ± 0.16 ^b	1.72 ± 0.02	2.39 ± 0.59	1.75 ± 0.46	***	***	***
γ-butyrolactone (mg/L)	7.10 ± 0.70	13.27 ± 0.47	7.20 ± 0.62	7.79 ± 1.46	5.04 ± 0.66	6.76 ± 2.59	6.57 ± 0.53 ^{b,†}	10.96 ± 0.64 ^{a,†}	10.05 ± 0.55 ^{a,†}	***	***	***
Acetaldehyde (mg/L)	8.00 ± 2.91 ^b	15.51 ± 4.97 ^{a,b}	22.88 ± 2.74 ^a	17.79 ± 4.52 ^a	11.87 ± 1.92 ^{a,b}	5.99 ± 2.45 ^b	15.94 ± 6.17	19.44 ± 4.24	14.26 ± 4.97	ns	ns	**
Ethyl acetate (mg/L)	47.48 ± 1.11 ^b	64.88 ± 7.15 ^a	59.74 ± 5.08 ^a	43.49 ± 2.44 ^b	33.49 ± 1.55 ^c	52.83 ± 4.01 ^a	47.04 ± 7.27	40.1 ± 5.56	48.57 ± 8.67	ns	**	ns
2-Phenethyl acetate (µg/L)	21.33 ± 0.58	24.00 ± 1.73	23.67 ± 4.16	31.67 ± 4.04	30.33 ± 4.93	47.00 ± 19.92	-	-	-	/	/	/

3.3. Basic Grape Juice and Yield Variables

In 2020 and 2022, statistically significant differences in TSS were observed between harvest dates (Table 2). However, differences in sugar concentrations in grape juice between harvest dates within the same experimental year were small (0.3–0.8 °Brix, Table 2), indicating that a plateau in sugar accumulation had been reached [12]. In the 2021 vintage, no significant increase in TSS concentration was observed from H1 to H3 (Table 2).

A notable decrease in berry weight between harvest dates was observed only in the 2020 vintage, which was characterized by substantial rainfall in June. This can explain the significant decrease in berry fresh weight from H1 to H3 in 2020, while berry weight remained stable in 2021. In contrast, in 2022, berry fresh mass increased from H2 to H3, which could be attributed to the rainfall before the harvest. Titratable acidity decreased significantly from H1 to H3, while the juice_pH value increased. Delaying harvest dates in our study did not have a significant influence on grapevine yield.

3.4. Wine Chemical Composition Analyses

An increase in ethanol concentration in wines from H1 to H3 was observed only in the 2022 vintage (Table 3). In 2021 ethanol concentrations remained unaffected by harvest date, whereas in 2020 an increase from H1 to H2 was observed, whereas concentrations in H3 were similar to those in H1 (Table 3).

Spectrophotometric analyses revealed differences in the concentration of total anthocyanins between harvest dates only in the 2020 vintage (Table 3). Total polyphenols in wines exhibited a similar trend to total anthocyanins. In the 2020 vintage, wines from the latest harvest date showed the highest anthocyanin and polyphenol concentration, whereas in 2021 and 2022 the maximum concentrations were generally reached at H2 and tended to decline by H3 (Table 3).

A total of 25 volatile compounds were analyzed for three consecutive years in wines made from grapes harvested on a weekly basis after reaching full maturity. One compound that generally exhibits decreasing trends with grape maturation is IBMP [13,30,54]. Also in our study in all three vintages, IBMP concentrations declined from H1 to H3 (Table 3). The highest IBMP concentration (6.57 ng/L) was measured in wines from H1 in the 2020 vintage.

Concentrations of 3MH varied between vintages, with overall levels ranging from several hundred to more than 1000 ng/L (Table 3). Significant differences among harvest dates were observed in all three vintages, with the lowest 3MH concentrations measured at H3. In 2020 and 2022, the highest 3MH values occurred at H1. By contrast, the other two thiols, 3MHA and 4MMP, were not significantly affected by harvest date (Table 3).

For C6 alcohols, a significant decrease in (Z)-3-hexenol from H1 to H3 was observed in 2021 and 2022, whereas a decrease was not significant in the 2020 vintage (Table 3). A similar pattern was also observed for 1-hexanol (Table 3, Figure 4B), supporting the general decline of green, herbaceous notes with delayed harvest [12,55]. Some differences in individual esters were observed in relation to harvest dates; however, they were vintage specific.

4. Discussion

This study examined the influence of sequential harvesting on the chemical composition of Merlot grape juice and wine across three vintages (2020–2022). Multivariate data analyses confirmed that vintage has the predominant effect on studied variables, while harvest date differentiated samples within each vintage, supporting the relevance of harvest timing for shaping grape and wine composition [3,15,44].

Across all vintages, only small differences in TSS were observed between early and late harvests. These findings align with previous studies indicating that during late ripening,

increases in TSS largely result from berry water loss as active sugar import into the berry declines [12,21,22,56]. Shahood et al. [21] showed that the cessation of sugar unloading during the ripening might be directly related to the cessation of berry growth, highlighting the close relationship between sugar transport and berry development. In our study, berry fresh mass was primarily driven by vintage effects, while the impact of harvest date was comparatively smaller. The highest berry mass was recorded in 2021, whereas in 2022 berry mass was lower, speculatively due to higher temperatures and lower precipitation, which is consistent with previous studies, indicating that berry weight is strongly influenced by water availability, especially around fruit set [55,57,58]. The observed increase in berry fresh mass in 2022 from H2 to H3 was likely associated with a rain event prior to harvest [58]. Furthermore, Rogiers and Holzapfel [55] reported that berries attaining higher maximum weights tend to exhibit greater subsequent weight loss under conditions of water deficit and drought, which may become particularly relevant when harvest is delayed under water-limited conditions.

Random forest analysis was used to identify the ten most important variables in juice and wine contributing to the discrimination between harvest dates. Juice TA (Figure 4A) was identified as the most important variable in our study to differentiate samples according to the harvest. The levels of TA in juice were consistently the lowest at H3. In contrast, pH values reached their highest values at H3 in 2020 and 2021, whereas harvest date had no significant effect on juice pH in 2022.

Small but significant differences in must TSS between harvest dates in 2020 and 2022 were observed and were followed by significant differences in wine ethanol concentrations. In 2021 no differences in ethanol content in wines from H1–H3 were observed (Table 3). The accumulation of anthocyanins during grape ripening is closely related to sugar dynamics, although this relationship is complex and strongly influenced by environmental conditions [18,59]. In our study, in 2020, a clear increase in total anthocyanin content in wine was observed with delayed harvest, whereas no such trend was observed in 2021 and 2022. In a previous study, we observed a plateau in anthocyanin biosynthesis that coincided with a plateau of sugar accumulation [11]. Moreover, berry anthocyanin, concentration during late ripening may also decrease due to degradation when exposed to high temperatures [60–62].

A similar pattern observed for total polyphenols further underscores the importance of harvest timing. These vintage-dependent differences highlight the strong influence of seasonal climate on phenolic development and extractability in Merlot wine [4,12,24].

Previous studies have linked herbaceous and green aroma attributes to IBMP and C6 alcohols (1-hexanol and (Z)-3-hexen-1-ol), which tend to be more abundant at earlier harvest dates [12,13,23,33]. In the present study, IBMP concentrations were higher in wines from H1 than from H3 across all three vintages. This is consistent with prior work indicating that harvest timing affects IBMP concentrations [13,63]. Although IBMP concentrations were below the reported perception threshold in red wines, its presence may still contribute to overall sensory perception [30]. Furthermore, IBMP concentrations are also affected by climatic conditions and viticultural practices [45], particularly canopy management and grape exposure [54,64,65].

(Z)-3-hexen-1-ol and 1-hexanol occurred at significantly higher concentrations in H1 than in H3 wines in the 2021 and 2022 vintages. (Z)-3-hexen-1-ol appears to be a varietal marker [12,55] and remains mainly unchanged during the yeast metabolic activity [28]. Its sensory properties are often described as fresh, fruity, and grassy [33]. However, in a mixture with 1-hexanol, α -ionone, and α -terpineol, it contributed to elevated perception of fresh red fruit and jammy red fruit [55], which are common sensory descriptors for earlier harvested grapes and wines [12]. Results of this study are confirmed with previous

work on Shiraz and Cabernet Sauvignon, where higher concentrations of (*Z*)-3-hexenol and (*E*)-3-hexenol were observed in Shiraz and Cabernet Sauvignon wines, respectively, at earlier harvest dates [27].

Although varietal thiols are typically associated with Sauvignon Blanc wines [35], contributing to the characteristic tropical fruit flavors, they are also present in wines of many other cultivars, including red wines [35]. It has been shown that the addition of 3MH and 3MHA to various red wines led to an enhanced perception of 'red fruit', 'blackcurrant', and 'tropical' characters [41]. Repeatedly, the lowest 3MH concentrations were measured in wines from H3 in all three vintages. This is in contrast to a significant increase in thiol precursors during grape ripening that was observed in several cultivars [20]. However, the conversion rate from precursors to varietal thiols during fermentation is low [66,67] and influenced by multiple fermentation factors [68].

Previous research on grape ripening and its influence on wine aromatic profile also identified few chemical markers derived from fermentation, with consistent trends across vintages and regions [12,13]. An increase in the concentrations of ethyl butyrate, propyl acetate, butyl acetate, isoamyl acetate, and phenylethyl acetate in Shiraz and γ -nonalactone in Cabernet Sauvignon with ripening was reported [12]. Quantified aroma compounds in our study did not exhibit explicit harvest date-specific trends, although some authors have reported increases in certain fermentation-derived compounds with delayed harvest [12,13,17]. This may indicate that fermentation-derived aroma compounds are shaped in part by grape composition [29] but remain largely governed by fermentation conditions and yeast metabolism [27].

While no sensory analysis was performed, the observed differences in wine chemical composition among harvest dates allow for cautious inference of potential sensory implications. As shown in previous studies [10,14,15,23], relationships between wine chemical composition and sensory expression are complex and often non-linear, as multiple compounds interact within the wine matrix and contribute to aroma perception, frequently at concentrations below individual sensory thresholds. In addition, the evolution of phenolic maturity and extractability during grape ripening of Merlot plays a central role in shaping wine color, mouthfeel, and overall sensory perception [24]. In the context of harvest timing, sequential harvest studies [9,12,13] have shown that changes in grape maturity and wine chemical composition are commonly associated with perceptible shifts in wine style, even when variations in individual wine chemical composition are relatively small.

Overall, the present study provides deeper insight into the ripening-associated changes in Merlot grapes and wines from a sub-Mediterranean climate. The findings further support the need to integrate multiple variables, such as juice TA, juice pH, phenolic maturity, aromatic development, and seasonal climatic conditions, when defining optimal harvest timing, instead of relying solely on TSS content. At the same time, these results should be interpreted within the scope of the present study, which focused on a single cultivar, Merlot, at one sub-Mediterranean site. Expanding this approach to additional cultivars, sites, and climatic contexts and integrating comprehensive chemical profiling with sensory evaluation will be essential to validate and generalize these results.

5. Conclusions

This three-year sequential harvest study demonstrates that both vintage and harvest date significantly influenced the chemical composition of Merlot juice and wine from a sub-Mediterranean site. Variance partitioning analysis confirmed that vintage was the dominant source of the variation, while harvest date differentiated grape and wine variables within each vintage.

Across vintages, delaying harvest from H1 to H3 was consistently associated with lower juice TA, while juice pH generally increased, supporting their robustness as indicators of physiological advancement during late ripening. In contrast, TSS differences were minor; therefore, TSS alone is insufficient as an indicator of physiological or aromatic maturity under these conditions.

Compounds associated with green sensory aroma attributes (IBMP, (Z)-3-hexenol, and 1-hexenol) showed decreasing trends with delayed harvest. Similarly, as harvest was delayed, the concentration of the thiol 3MH decreased significantly. Enhancements in anthocyanin and phenolic contents, however, were observed only at individual vintages, highlighting the environmental dependence of phenolic development. Other fermentation-derived volatiles showed mainly compound- and vintage-specific responses, reflecting the complexity of volatile formation pathways and the important influence of interannual climatic variability.

Within this framework, the present study provides important insights into harvest date-driven shifts in volatile composition in Merlot wines. Despite the reduction in herbaceous and green related aroma compounds achieved by delaying harvest for 7 to 14 days, gains in phenolic maturity are uncertain and must be carefully balanced against the elevated dehydration risk during warm or dry vintage. Together, these findings underscore the need for a multifactorial framework integrating harvest-related variables when defining Merlot wine style under variable sub-Mediterranean climatic conditions.

Author Contributions: Conceptualization, F.Č.; methodology, A.J.K., F.Č., and K.Š.; software, A.J.K., K.Š., and M.P.; validation, A.J.K. and K.Š.; formal analysis, A.J.K.; investigation, A.J.K. and A.Š.; resources, A.Š.; data curation, A.J.K. and K.Š.; writing—original draft preparation, K.Š. and A.J.K.; writing—review and editing, F.Č., M.P., and A.Š.; visualization, K.Š.; supervision, F.Č.; project administration, A.J.K.; funding acquisition, F.Č. All authors have read and agreed to the published version of the manuscript.

Funding: This research was funded by the Ministry of agriculture, forestry, and food of the republic of Slovenia, grants numbers 2330-20-000157, 2330-21-000025, and 2330-22-000010, The APC was funded by the Slovenian Research and Innovation Agency (ARIS), grant number P4-0133.

Data Availability Statement: The original data presented in the study are openly available from the corresponding author upon request.

Acknowledgments: We thank H. Baša Česnik and T. Sket, who helped with GC-MS and GC-FID analysis, and Boštjan Saje, who helped with lab-scale fermentations.

Conflicts of Interest: The authors declare no conflicts of interest. The funders had no role in the design of the study; in the collection, analyses, or interpretation of data; in the writing of the manuscript; or in the decision to publish the results.

Abbreviations

The following abbreviations are used in this manuscript:

3MH	3-mercapto hexanol
3MHA	3-mercaptohexyl acetate
4MMP	4-mercapto-4-methyl pentan-2-ol
DAA	Days after anthesis
GDD10	Growing degrees days calculated using 10 °C as the baseline temperature
H1	Harvest time point 1
H2	Harvest time point 2
H3	Harvest time point 3
EEFAs	Ethyl esters of fatty acids
IBMP	3-isobutyl-2-methoxypyrazine

IPMP	3-isopropyl-2-methoxypyrazine
MLF	Malolactic fermentation
TA	Titrateable acidity
TSS	Total soluble solids
VPA	Variance partitioning analyses
YAN	Yeast assimilable nitrogen

References

- Lin, J.; Massonnet, M.; Cantu, D. The Genetic Basis of Grape and Wine Aroma. *Hortic. Res.* **2019**, *6*, 81. [[CrossRef](#)]
- Jiang, B.; Xi, Z.; Luo, M.; Zhang, Z. Comparison on Aroma Compounds in Cabernet Sauvignon and Merlot Wines from Four Wine Grape-Growing Regions in China. *Food Res. Int.* **2013**, *51*, 482–489. [[CrossRef](#)]
- Van Leeuwen, C.; Barbe, J.-C.; Darriet, P.; Geffroy, O.; Gomès, E.; Guillaumie, S.; Helwi, P.; Laboyrie, J.; Lytra, G.; Le Menn, N.; et al. Recent Advancements in Understanding the Terroir Effect on Aromas in Grapes and Wines. *OENO One* **2020**, *54*, 985–1006. [[CrossRef](#)]
- Casassa, L.F.; Beaver, C.W.; Mireles, M.; Larsen, R.C.; Hopfer, H.; Heymann, H.; Harbertson, J.F. Influence of Fruit Maturity, Maceration Length, and Ethanol Amount on Chemical and Sensory Properties of Merlot Wines. *Am. J. Enol. Vitic.* **2013**, *64*, 437–449. [[CrossRef](#)]
- Du Plessis, C.S. Optimum Maturity and Quality Parameters in Grapes: A Review. *S. Afr. J. Enol. Vitic.* **1984**, *5*, 34–42. [[CrossRef](#)]
- Gomez, E.; Martinez, A.; Laencina, J. Changes in Volatile Compounds during Maturation of Some Grape Varieties. *J. Sci. Food Agric.* **1995**, *67*, 229–233. [[CrossRef](#)]
- Rice, S.; Tursumbayeva, M.; Clark, M.; Greenlee, D.; Dharmadhikari, M.; Fennell, A.; Koziel, J.A. Effects of Harvest Time on the Aroma of White Wines Made from Cold-Hardy Brianna and Frontenac Gris Grapes Using Headspace Solid-Phase Microextraction and Gas Chromatography-Mass Spectrometry-Olfactometry. *Foods* **2019**, *8*, 29. [[CrossRef](#)]
- Trujillo, M.; Bely, M.; Albertin, W.; Masneuf-Pomarède, I.; Colonna-Ceccaldi, B.; Marullo, P.; Barbe, J.-C. Impact of Grape Maturity on Ester Composition and Sensory Properties of Merlot and Tempranillo Wines. *J. Agric. Food Chem.* **2022**, *70*, 11520–11530. [[CrossRef](#)]
- Allamy, L.; Van Leeuwen, C.; Pons, A. Impact of Harvest Date on Aroma Compound Composition of Merlot and Cabernet-Sauvignon Must and Wine in a Context of Climate Change: A Focus on Cooked Fruit Molecular Markers. *OENO One* **2023**, *57*, 99–112. [[CrossRef](#)]
- Lu, H.-C.; Tian, M.-B.; Han, X.; Shi, N.; Li, H.-Q.; Cheng, C.-F.; Chen, W.; Li, S.-D.; He, F.; Duan, C.-Q.; et al. Vineyard Soil Heterogeneity and Harvest Date Affect Volatolomics and Sensory Attributes of Cabernet Sauvignon Wines on a Meso-Terroir Scale. *Food Res. Int.* **2023**, *174*, 113508. [[CrossRef](#)]
- Deloire, A. Berry Ripening and Wine Aroma. *Pract. Winery Vineyard J.* **2013**, *2013*, 1–2.
- Antalick, G.; Šuklje, K.; Blackman, J.W.; Schmidtke, L.M.; Deloire, A. Performing Sequential Harvests Based on Berry Sugar Accumulation (Mg/Berry) to Obtain Specific Wine Sensory Profiles. *OENO One* **2021**, *55*, 131–146. [[CrossRef](#)]
- Bindon, K.; Varela, C.; Kennedy, J.; Holt, H.; Herderich, M. Relationships between Harvest Time and Wine Composition in *Vitis vinifera* L. Cv. Cabernet Sauvignon 1. Grape and Wine Chemistry. *Food Chem.* **2013**, *138*, 1696–1705. [[CrossRef](#)] [[PubMed](#)]
- Olarte Mantilla, S.M.; Collins, C.; Iland, P.G.; Kidman, C.M.; Ristic, R.; Hasted, A.; Jordans, C.; Bastian, S.E.P. Relationships between Grape and Wine Sensory Attributes and Compositional Measures of Cv. Shiraz. *Am. J. Enol. Vitic.* **2015**, *66*, 177–186. [[CrossRef](#)]
- Schmidtke, L.M.; Antalick, G.; Šuklje, K.; Blackman, J.W.; Bocard, J.; Deloire, A. Cultivar, Site or Harvest Date: The Gordian Knot of Wine Terroir. *Metabolomics* **2020**, *16*, 52. [[CrossRef](#)]
- Marais, J.; Van Wyk, C.J. Effect of Grape Maturity and Juice Treatments on Terpene Concentrations and Wine Quality of *Vitis vinifera* L. Cv. Weisser Riesling and Bukettraube. *SAJEV* **1986**, *7*, 26–35. [[CrossRef](#)]
- Škrab, D.; Sivilotti, P.; Comuzzo, P.; Voce, S.; Cisilino, D.; Carlin, S.; Arapitsas, P.; Masuero, D.; Vrhovsek, U. Influence of Harvest Date on Multi-Targeted Metabolomic Profile and Sensory Attributes of Ribolla Gialla Base and Sparkling Wines. *OENO One* **2024**, *58*, 1–18. [[CrossRef](#)]
- Castellarin, S.D.; Pfeiffer, A.; Sivilotti, P.; Degan, M.; Peterlunger, E.; Di Gaspero, G. Transcriptional Regulation of Anthocyanin Biosynthesis in Ripening Fruits of Grapevine under Seasonal Water Deficit. *Plant Cell Environ.* **2007**, *30*, 1381–1399. [[CrossRef](#)]
- Mori, K.; Goto-Yamamoto, N.; Kitayama, M.; Hashizume, K. Loss of Anthocyanins in Red-Wine Grape under High Temperature. *J. Exp. Bot.* **2007**, *58*, 1935–1945. [[CrossRef](#)]
- Cerreti, M.; Esti, M.; Benucci, I.; Liburdi, K.; De Simone, C.; Ferranti, P. Evolution of S-Cysteinylation and S-Glutathionylation Thiol Precursors during Grape Ripening of *Vitis vinifera* L. Cvs Grechetto, Malvasia Del Lazio and Sauvignon Blanc: Thiol Precursors in Grape. *Aust. J. Grape Wine Res.* **2015**, *21*, 411–416. [[CrossRef](#)]

21. Shahood, R.; Torregrosa, L.; Savoi, S.; Romieu, C. First Quantitative Assessment of Growth, Sugar Accumulation and Malate Breakdown in a Single Ripening Berry. *OENO One* **2020**, *54*, 1077–1092. [[CrossRef](#)]
22. Deloire, A. Physiological Indicators to Predict Harvest Date and Wine Style. In Proceedings of the Physiological Indicators to Predict Harvest Date and Wine Style, Sydney, NSW, Australia, 13 July 2013; Volume 2013, pp. 47–50.
23. Šuklje, K.; Carlin, S.; Stanstrup, J.; Antalick, G.; Blackman, J.W.; Meeks, C.; Deloire, A.; Schmidtke, L.M.; Vrhovsek, U. Unravelling Wine Volatile Evolution during Shiraz Grape Ripening by Untargeted HS-SPME-GC × GC-TOFMS. *Food Chem.* **2019**, *277*, 753–765. [[CrossRef](#)] [[PubMed](#)]
24. Allegro, G.; Bautista-Ortín, A.B.; Gómez-Plaza, E.; Pastore, C.; Valentini, G.; Filippetti, I. Impact of Flavonoid and Cell Wall Material Changes on Phenolic Maturity in Cv. Merlot (*Vitis vinifera* L.). *Am. J. Enol. Vitic.* **2018**, *69*, 417–421. [[CrossRef](#)]
25. Allegro, G.; Pastore, C.; Valentini, G.; Filippetti, I. The Evolution of Phenolic Compounds in *Vitis vinifera* L. Red Berries during Ripening: Analysis and Role on Wine Sensory—A Review. *Agronomy* **2021**, *11*, 999. [[CrossRef](#)]
26. Šuklje, K.; Zhang, X.; Antalick, G.; Clark, A.C.; Deloire, A.; Schmidtke, L.M. Berry Shriveling Significantly Alters Shiraz (*Vitis vinifera* L.) Grape and Wine Chemical Composition. *J. Agric. Food Chem.* **2016**, *64*, 870–880. [[CrossRef](#)]
27. Antalick, G.; Šuklje, K.; Blackman, J.W.; Meeks, C.; Deloire, A.; Schmidtke, L.M. Influence of Grape Composition on Red Wine Ester Profile: Comparison between Cabernet Sauvignon and Shiraz Cultivars from Australian Warm Climate. *J. Agric. Food Chem.* **2015**, *63*, 4664–4672. [[CrossRef](#)]
28. Swiegers, J.H.; Bartowsky, E.J.; Henschke, P.A.; Pretorius, I.S. Yeast and Bacterial Modulation of Wine Aroma and Flavour. *Aust. J. Grape Wine Res.* **2005**, *11*, 139–173. [[CrossRef](#)]
29. Boss, P.; Pearce, A.; Zhao, Y.; Nicholson, E.; Dennis, E.; Jeffery, D. Potential Grape-Derived Contributions to Volatile Ester Concentrations in Wine. *Molecules* **2015**, *20*, 7845–7873. [[CrossRef](#)]
30. Roujou De Boubée, D.; Van Leeuwen, C.; Dubourdieu, D. Organoleptic Impact of 2-Methoxy-3-Isobutylpyrazine on Red Bordeaux and Loire Wines. Effect of Environmental Conditions on Concentrations in Grapes during Ripening. *J. Agric. Food Chem.* **2000**, *48*, 4830–4834. [[CrossRef](#)]
31. Previtali, P.; Dokoozlian, N.; Capone, D.L.; Wilkinson, K.L.; Ford, C.M. Exploratory Study of Sugar and C6 Compounds in Single Berries of Grapevine (*Vitis vinifera* L.) Cv. Cabernet Sauvignon throughout Ripening. *Aust. J. Grape Wine Res.* **2021**, *27*, 194–205. [[CrossRef](#)]
32. Boss, P.K.; Böttcher, C.; Davies, C. Various Influences of Harvest Date and Fruit Sugar Content on Different Wine Flavor and Aroma Compounds. *Am. J. Enol. Vitic.* **2014**, *65*, 341–353. [[CrossRef](#)]
33. Kalua, C.M.; Boss, P.K. Evolution of Volatile Compounds during the Development of Cabernet Sauvignon Grapes (*Vitis vinifera* L.). *J. Agric. Food Chem.* **2009**, *57*, 3818–3830. [[CrossRef](#)] [[PubMed](#)]
34. Allen, M.S.; Lacey, M.J.; Harris, R.L.N.; Brown, W.V. Contribution of Methoxypyrazines to Sauvignon Blanc Wine Aroma. *Am. J. Enol. Vitic.* **1991**, *42*, 109–112. [[CrossRef](#)]
35. Roland, A.; Schneider, R.; Razungles, A.; Cavelier, F. Varietal Thiols in Wine: Discovery, Analysis and Applications. *Chem. Rev.* **2011**, *111*, 7355–7376. [[CrossRef](#)]
36. Darriet, P.; Tominaga, T.; Lavigne, V.; Boidron, J.; Dubourdieu, D. Identification of a Powerful Aromatic Component of *Vitis vinifera* L. Var. Sauvignon Wines: 4-mercapto-4-methylpentan-2-one. *Flavour. Fragr. J.* **1995**, *10*, 385–392. [[CrossRef](#)]
37. Tominaga, T.; Darriet, P.; Dubourdieu, D. Identification of 3-Mercaptohexyl Acetate in Sauvignon Wine, a Powerful Aromatic Compound Exhibiting Box-Tree Odor. *Vitis* **1996**, *35*, 207–210.
38. Tominaga, T.; Furrer, A.; Henry, R.; Dubourdieu, D. Identification of New Volatile Thiols in the Aroma of *Vitis vinifera* L. Var. Sauvignon Blanc Wines. *Flavour. Fragr. J.* **1998**, *13*, 159–162. [[CrossRef](#)]
39. Rigou, P.; Triay, A.; Razungles, A. Influence of Volatile Thiols in the Development of Blackcurrant Aroma in Red Wine. *Food Chem.* **2014**, *142*, 242–248. [[CrossRef](#)]
40. Siebert, T.; Francis, L.; Pisaniello, L.; Melzer, S.; Bey, L.; Watson, F.; Espinase Nandorfy, D.; Cordente, T. Do Varietal Thiols Matter in Red Wine? *AWRI Tech. Rev.* **2019**, *2019*, 10–15.
41. Siebert, T.; Solomon, M.; Pisaniello, L.; Espinase Nandorfy, D.; Bilogrevic, E.; Wat-Son, F.; Cordente, T.; Francis, L.; Hixson, J. Tropical Polyfunctional Thiols and Their Role in Australian Red Wines. In Proceedings of the OENO Macrowine 2023, Bordeaux, France, 10 July 2023; Volume 2023.
42. Lorenz, D.H.; Eichhorn, K.W.; Bleiholder, H.; Klose, R.; Meier, U.; Weber, E. Growth Stages of the Grapevine: Phenological Growth Stages of the Grapevine (*Vitis vinifera* L. ssp. *vinifera*)—Codes and Descriptions According to the Extended BBCH Scale. *Aust. J. Grape Wine Res.* **1995**, *1*, 100–103. [[CrossRef](#)]
43. Hall, A.; Jones, G.V. Spatial Analysis of Climate in Winegrape-Growing Regions in Australia. *Aust. J. Grape Wine Res.* **2010**, *16*, 389–404. [[CrossRef](#)]
44. Tonietto, J.; Carbonneau, A. A Multicriteria Climatic Classification System for Grape-Growing Regions Worldwide. *Agric. For. Meteorol.* **2004**, *124*, 81–97. [[CrossRef](#)]
45. Mihelčič, A.; Vanzo, A.; Sivilotti, P.; Vrščaj, B.; Lisjak, K. An Investigation of Vine Water Status as a Major Factor in the Quality of Merlot Wine Produced in Terraced and Non-Terraced Vineyards in the Vipava Valley, Slovenia. *OENO One* **2023**, *57*, 231–246. [[CrossRef](#)]

46. Rigo, A.; Vianello, F.; Clementi, G.; Rossetto, M.; Scarpa, M.; Vrhovšek, U.; Mattivi, F. Contribution of Proanthocyanidins to the Peroxy Radical Scavenging Capacity of Some Italian Red Wines. *J. Agric. Food Chem.* **2000**, *48*, 1996–2002. [[CrossRef](#)] [[PubMed](#)]
47. Tominaga, T.; Dubourdieu, D. A Novel Method for Quantification of 2-Methyl-3-Furanthiol and 2-Furanmethanethiol in Wines Made from *Vitis vinifera* Grape Varieties. *J. Agric. Food Chem.* **2006**, *54*, 29–33. [[CrossRef](#)] [[PubMed](#)]
48. Jenko, M.; Lisjak, K.; Košmerl, T.; Čuš, F. The Influence of Yeast Strain Combinations on the Quality of Sauvignon Blanc Wine. *FSTR* **2013**, *19*, 7–15. [[CrossRef](#)]
49. Martelanc, M.; Slaghenaufi, D.; Radovanović Vukajlović, T.; Martin Rojas, D.A.; Suklje, K.; Sternad Lemut, M.; Mozetič Vodopivec, B.; Butinar, L.; Antalick, G. A Unique Mixture of Monoterpenes and Volatile Phenols Characterises Zelen Wine's Aromatic Profile. *OENO One* **2025**, *59*. [[CrossRef](#)]
50. Šuklje, K.; Čuš, F. Modulation of Welschriesling Wine Volatiles through the Selection of Yeast and Lactic Acid Bacteria. *OENO One* **2021**, *55*, 245–260. [[CrossRef](#)]
51. Šuklje, K.; Lisjak, K.; Baša Česnik, H.; Janeš, L.; Du Toit, W.; Coetzee, Z.; Vanzo, A.; Deloire, A. Classification of Grape Berries According to Diameter and Total Soluble Solids to Study the Effect of Light and Temperature on Methoxypyrazine, Glutathione, and Hydroxycinnamate Evolution during Ripening of Sauvignon Blanc (*Vitis vinifera* L.). *J. Agric. Food Chem.* **2012**, *60*, 9454–9461. [[CrossRef](#)]
52. Bavčar, D.; Česnik, H.B. Validation of the Method for the Determination of Some Wine Volatile Compounds. *Acta Agric. Slov.* **2011**, *97*, 285–293. [[CrossRef](#)]
53. Bavčar, D.; Baša Česnik, H.; Čuš, F.; Košmerl, T. The Influence of Skin Contact during Alcoholic Fermentation on the Aroma Composition of Ribolla Gialla and Malvasia Istriana *Vitis vinifera* (L.) Grape Wines. *Int. J. Food Sci. Tech.* **2011**, *46*, 1801–1808. [[CrossRef](#)]
54. Ryona, I.; Pan, B.S.; Intrigliolo, D.S.; Lakso, A.N.; Sacks, G.L. Effects of Cluster Light Exposure on 3-Isobutyl-2-Methoxypyrazine Accumulation and Degradation Patterns in Red Wine Grapes (*Vitis vinifera* L. Cv. Cabernet Franc). *J. Agric. Food Chem.* **2008**, *56*, 10838–10846. [[CrossRef](#)] [[PubMed](#)]
55. Rogiers, S.Y.; Holzzapfel, B.P. The Plasticity of Berry Shrivelling in “Shiraz”: A Vineyard Survey. *VITIS J. Grapevine Res.* **2015**, *54*, 1–8. [[CrossRef](#)]
56. Lang, A.; Thorpe, M.R. Xylem, Phloem and Transpiration Flows in a Grape: Application of a Technique for Measuring the Volume of Attached Fruits to High Resolution Using Archimedes' Principle. *J. Exp. Bot.* **1989**, *40*, 1069–1078. [[CrossRef](#)]
57. Ojeda, H.; Deloire, A.; Carbonneau, A. Influence of Water Deficits on Grape Berry Growth. *VITIS J. Grapevine Res.* **2015**, *40*, 141–145. [[CrossRef](#)]
58. Rogiers, S.Y.; Greer, D.H.; Liu, Y.; Baby, T.; Xiao, Z. Impact of Climate Change on Grape Berry Ripening: An Assessment of Adaptation Strategies for the Australian Vineyard. *Front. Plant Sci.* **2022**, *13*, 1094633. [[CrossRef](#)]
59. He, F.; Liang, N.-N.; Mu, L.; Pan, Q.-H.; Wang, J.; Reeves, M.J.; Duan, C.-Q. Anthocyanins and Their Variation in Red Wines I. Monomeric Anthocyanins and Their Color Expression. *Molecules* **2012**, *17*, 1571–1601. [[CrossRef](#)]
60. Pérez-Magariño, S.; González-San José, M.L. Polyphenols and Colour Variability of Red Wines Made from Grapes Harvested at Different Ripeness Grade. *Food Chem.* **2006**, *96*, 197–208. [[CrossRef](#)]
61. Jedyi, H.; Naamani, K.; Ait Elkoch, A.; Dihazi, A.; El Alaoui El Fels, A.; Arkize, W. First Study on Technological Maturity and Phenols Composition during the Ripeness of Five *Vitis vinifera* L. Grape Varieties in Morocco. *Sci. Hort.* **2019**, *246*, 390–397. [[CrossRef](#)]
62. Rolle, L.; Torchio, F.; Zeppa, G.; Gerbi, V. Anthocyanin Extractability Assessment of Grape Skins by Texture Analysis. *OENO One* **2008**, *42*, 157. [[CrossRef](#)]
63. Ryona, I.; Pan, B.S.; Sacks, G.L. Rapid Measurement of 3-Alkyl-2-Methoxypyrazine Content of Winegrapes to Predict Levels in Resultant Wines. *J. Agric. Food Chem.* **2009**, *57*, 8250–8257. [[CrossRef](#)]
64. Sivilotti, P.; Herrera, J.C.; Lisjak, K.; Baša Česnik, H.; Sabbatini, P.; Peterlunger, E.; Castellarin, S.D. Impact of Leaf Removal, Applied Before and After Flowering, on Anthocyanin, Tannin, and Methoxypyrazine Concentrations in 'Merlot' (*Vitis vinifera* L.) Grapes and Wines. *J. Agric. Food Chem.* **2016**, *64*, 4487–4496. [[CrossRef](#)]
65. Scheiner, J.J.; Sacks, G.L.; Pan, B.; Ennahli, S.; Tarlton, L.; Wise, A.; Lerch, S.D.; Vanden Heuvel, J.E. Impact of Severity and Timing of Basal Leaf Removal on 3-Isobutyl-2-Methoxypyrazine Concentrations in Red Winegrapes. *Am. J. Enol. Vitic.* **2010**, *61*, 358–364. [[CrossRef](#)]
66. Murat, M.-L.; Tominaga, T.; Dubourdieu, D. Assessing the Aromatic Potential of Cabernet Sauvignon and Merlot Musts Used to Produce Rose Wine by Assaying the Cysteinylated Precursor of 3-Mercaptohexan-1-Ol. *J. Agric. Food Chem.* **2001**, *49*, 5412–5417. [[CrossRef](#)]
67. Cordente, A.G.; Curtin, C.D.; Solomon, M.; Kulcsar, A.C.; Watson, F.; Pisaniello, L.; Schmidt, S.A.; Espinase Nandorfy, D. Modulation of Volatile Thiol Release during Fermentation of Red Musts by Wine Yeast. *Processes* **2022**, *10*, 502. [[CrossRef](#)]
68. Pinu, F.R.; Edwards, P.J.B.; Jouanneau, S.; Kilmartin, P.A.; Gardner, R.C.; Villas-Boas, S.G. Sauvignon Blanc Metabolomics: Grape Juice Metabolites Affecting the Development of Varietal Thiols and Other Aroma Compounds in Wines. *Metabolomics* **2014**, *10*, 556–573. [[CrossRef](#)]

Disclaimer/Publisher's Note: The statements, opinions and data contained in all publications are solely those of the individual author(s) and contributor(s) and not of MDPI and/or the editor(s). MDPI and/or the editor(s) disclaim responsibility for any injury to people or property resulting from any ideas, methods, instructions or products referred to in the content.